

# IN-SITU BULK RESISTIVITY RATIO MEASUREMENT ON DOUBLE QUARTER WAVE CRAB CAVITIES

N. Shipman<sup>1 2\*</sup>, G. Burt, J. Mitchell<sup>1,2</sup>, Lancaster University, Lancaster, UK

A. Castilla, K. Chahín<sup>3</sup>, A. MacPherson, CERN, Geneva, Switzerland

I. Ben-Zvi, Brookhaven National Laboratory, Upton, USA

<sup>1</sup>also at Cockcroft Institute, Daresbury, UK

<sup>2</sup>also at CERN, Geneva, Switzerland

<sup>3</sup>also at DCI-UG, Guanajuato, Mexico

## Abstract

A four wire measurement was used to measure the bulk RRR on two DQW Crab Cavities. The measurement procedure is explained and the values obtained for each cavity are compared together with the values obtained from Niobium samples of the same stock from which the cavities were manufactured. Measurement errors are carefully analysed and further improvements to the measurement procedure are suggested.

## INTRODUCTION

### Introduction to HL-LHC and Crab Cavities

High-Luminosity-LHC [1], HL-LHC, is a project to upgrade the Large Hadron Collider [2], LHC, by increasing the luminosity by a factor of 10. This will allow more accurate measurements of newly discovered particles and allow the discovery of rare processes which are below the current sensitivity level of the LHC.

In order to achieve the requisite increase in luminosity it is necessary to utilise crab cavities. Crab cavities rotate the particle bunches about an axis perpendicular to the plane containing both beam axes in such a way as to almost completely counteract the geometric luminosity reduction which would otherwise occur as a result of the non-perfect overlap of the colliding bunches [3] as shown in Fig.1.

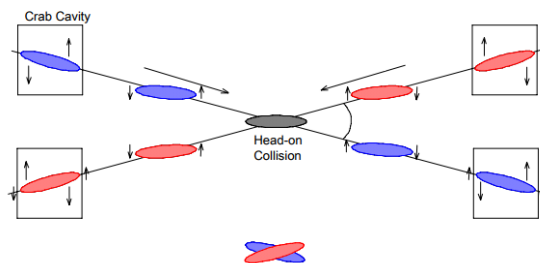
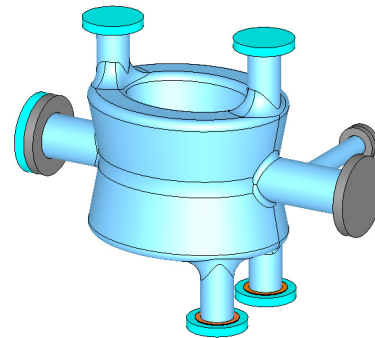


Figure 1: For each beam crab cavities upstream and downstream of the interaction point rotate the bunches to reduce the luminosity loss due to the non-perfect overlap that would otherwise be caused by the crossing angle.

Three prototype designs of crab cavities for the HL-LHC project were built. The double quarter wave crab cavity,

\* nicholas.shipman@cern.ch



(a) A 3D model of the DQW SPS crab cavity.



(b) Photograph of the DQW SPS crab cavity without helium tank.

Figure 2: DQW SPS crab cavity.

DQW [4], the radio frequency dipole crab cavity [5], RFD and the UK four rod cavity [6], UK4R. For HL-LHC, the DQW and RFD were selected to be installed in the LHC and the DQW cavity will also first be tested in the super proton synchrotron, SPS. Two "DQW SPS" cavities have been constructed for this purpose and prior to testing in the SPS they have undergone cold testing both at JLAB [7] and at CERN [8]. Figure 2 shows both a 3D representation in Sub-Fig.2a and a photograph of a completed DQW SPS cavity in Sub-Fig.2b, before the helium tank was installed.

### Introduction to RRR

The residual resistivity ratio, RRR, of a metal is defined as the ratio of the resistivity at 300K to the resistivity at a low temperature just above the superconducting transition. [9]

$$RRR = \frac{\text{resistivity 300 K}}{\text{residual resistivity at low temperature (normal state)}} \quad (1)$$

Here 'low temperature' is defined as 10 K. The RRR of the surface is usually different to that of the bulk. In this paper we are concerned with the bulk RRR. The Franz-Weidmann law [10] [11] states:

$$\frac{\kappa}{\sigma} = LT \quad (2)$$

where  $\kappa$  is the thermal conductivity,  $\sigma$  is the electrical conductivity,  $T$  is the temperature and  $L$  is a constant of proportionality known as the Lorentz number. As a metal with a high RRR has a higher electrical conductivity at low temperatures so too will it have a high thermal conductivity. Therefore manufacturing superconducting bulk Niobium cavities from Niobium which has a high RRR is desirable as the increased thermal conductivity will: lead to a cooler inside surface; increase the  $Q_0$  (intrinsic quality factor) for a given field level; and suppress thermal breakdown allowing higher field levels to be achieved. [12] A higher  $Q_0$  will decrease the heat dissipation on the cavity surface which is important for the cryomodule [13] design.

The DQW SPS cavities were made from Niobium which had been certified by the manufacturer to have a RRR greater than 300 this was also verified independently at CERN. However steps in the cavity fabrication process, particularly electron beam welding and heat treatments are known to have the potential to degrade the RRR. [14] The only way to know the RRR of the cavity therefore, is to measure the RRR of the cavity itself as part of the cold test.

### MEASURED RRR OF SAMPLES

Six samples were cut from the same sheet of Niobium used to make the DQW SPS 2 cavity. The sheet was 4 mm thick and the samples machined from it were  $122 \times 2 \times 2$  mm in size. A buffered chemical polish, BCP, was performed to attain a final size of  $121.9 \times 1.9 \times 1.9$  mm. Three of the samples underwent the same heat treatment at the same time and in the same oven as the cavity whereas the other three did not. All six samples then had their RRR measured in the cryolab at CERN.<sup>1</sup>

This measurement was also done using a four wire technique. Despite the reduced length, the smaller cross section of the samples compared to the full cavity leads to a resistance which is nearly two orders of magnitude greater. This coupled with shorter measurement cables and a less noisy environment more easily facilitate accurate measurements than the measurements on the cavity itself.

The results of the non heat treated samples are shown in Tab.1 and the results of the heat treated samples are shown in Tab.2. The error in the RRR for each sample is calculated from the error in the resistance at 10 K and 300 K (not shown).

<sup>1</sup> These measurements were not made by the authors, please see acknowledgements.

Table 1: Measured Bulk RRR of Samples without Heat Treatment

	Sample 1	Sample 2	Sample 3
10 K	$1.22 \times 10^{-5} \Omega$	$1.18 \times 10^{-5} \Omega$	$1.21 \times 10^{-5} \Omega$
300 K	$4.34 \times 10^{-3} \Omega$	$4.28 \times 10^{-3} \Omega$	$4.44 \times 10^{-3} \Omega$
RRR	$355.7 \pm 7.8$	$362.7 \pm 7.3$	$366.9 \pm 12.9$

Table 2: Measured Bulk RRR of Heat Treated Samples

	Sample 1	Sample 2	Sample 3
10 K	$1.70 \times 10^{-5} \Omega$	$1.68 \times 10^{-5} \Omega$	$1.65 \times 10^{-5} \Omega$
300 K	$4.47 \times 10^{-3} \Omega$	$4.51 \times 10^{-3} \Omega$	$4.41 \times 10^{-3} \Omega$
RRR	$262.9 \pm 4.9$	$268.5 \pm 6.3$	$267.3 \pm 5.1$

The weighted mean and standard deviation of the RRR for the non heat treated samples was  $361 \pm 10$  whereas for the heat treated samples it was  $266 \pm 5$ .

### EXPERIMENTAL SETUP

The resistance of the cavity was measured at different temperatures using a four-wire technique as shown in Fig.3. The current carrying leads and the voltage pick up leads were each a shielded twisted pair in the same cable which itself was shielded. Separate grounds were used for the cable and each of the pairs to reduce the noise on the voltage measurement leads. Each lead and ground was passed to the inside of the cryostat with a "dsub" type feedthrough whilst maintaining electrical isolation from the cryostat. Due to the small cross section of the conductor the current supplied to the DQW SPS 1 cavity was limited to 200 mA to avoid any risk of melting the wire. For the DQW SPS 2 cavity it was decided to increase this limit to 800 mA, reducing the measurement error albeit by increasing the risk of melting the leads.

One current lead was fastened to each beam port flange using a bolt and nut to ensure a good connection. The voltage measurement leads were attached to the beam pipe itself with aluminium tape rather than to the steel flange to ensure only the voltage drop across the Niobium was measured. Both the current and voltage leads followed the contours of

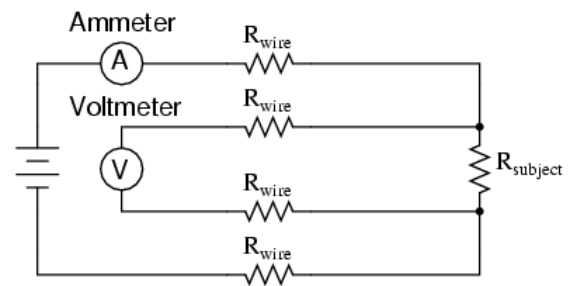


Figure 3: Schematic representation of a 4-wire measurement.

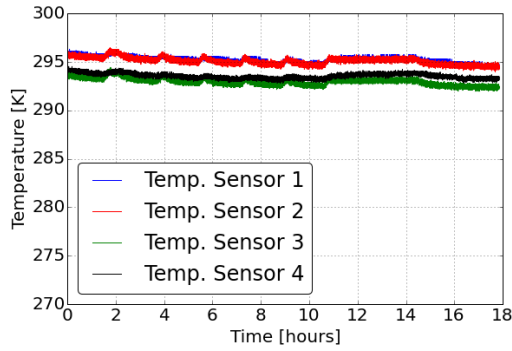


Figure 4: Measured temperature of cavity from four different sensors before cool-down.

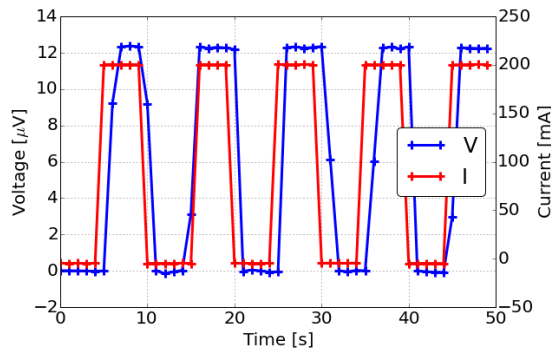


Figure 5: A sample of the recorded voltage and current data for SPS1 at 300 K.

the cavity closely to minimise the mutual inductance of the measurement setup to its surroundings. It was necessary however to leave a small amount of slack in the leads to account for the greater thermal contraction of the copper leads compared to the Niobium cavity and thus avoid the attachment points pulling off the surface of the cavity.

Four Cernox 1050 HT sensors [15] were attached to the cavity surface to measure the temperature. The sensors have an accuracy of less than 40 K at temperatures between 1.4 K and 300 K. For the analysis the cavity temperature was taken to be that of the sensor in the middle of the cavity, but if the temperature gradient across the cavity was greater than 3 K the results were discarded.

## RESULTS AND ANALYSIS

All the plots shown in this section are for the DQW SPS 1 cavity, exactly the same analysis was carried out for the DQW SPS 2 cavity the results of which are shown and discussed in the following section.

Figure 4 shows the cavity temperature for a period of  $\approx 18$  hours before the cool down started. Throughout this time a current of 200 mA with a 50% duty cycle and period of 10 s was applied to the cavity and the voltage drop across the cavity was recorded. A snap shot of the current and voltage data recorded is shown in Fig.5.

ISBN 978-3-95450-191-5

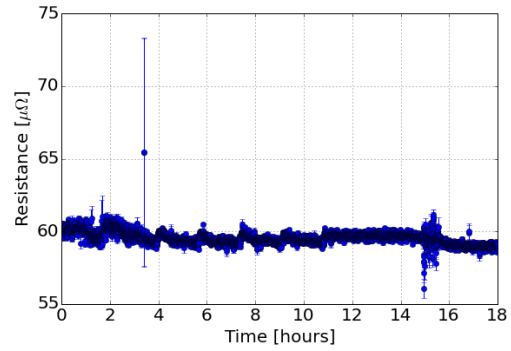


Figure 6: The resistance calculated by dividing the change in voltage by the change in current. Each 'sample' corresponds to the resistance calculated from the voltage change for each change in current.

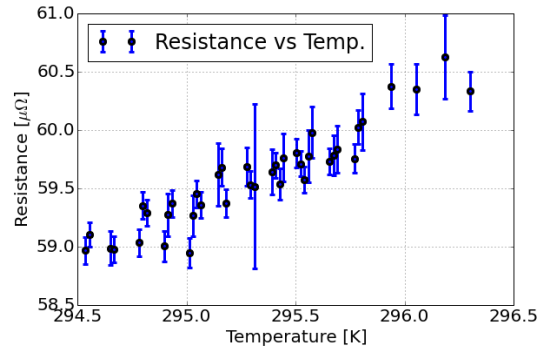


Figure 7: The weighted mean of the cavity resistance calculated at each unique temperature.

Due to thermoelectric currents, instrument calibration errors, ground noise and instrument drift the resistance cannot be calculated directly as  $\frac{V}{I}$ . Instead for each change in current the resistance calculated as:  $R = \frac{\Delta V}{\Delta I}$ .

Figure 6 shows the calculated resistance and error at high temperature. The resistance varies by a non-negligible amount due to small temperature changes of the cavity. Resistances at the same temperature were combined to yield a set of weighted means and standard deviations of resistance for a range of temperatures as shown in Fig. 7.

A linear regression of the resistances calculated at high temperature is made to 300 K as shown in Fig. 8. The error in the fitting parameters is calculated to allow the standard deviation of the resistance at 300 K to be determined.

To enhance cavity performance, after the rapid cooldown a thermal cycle is performed [16], during which the cavity is warmed up to above 10K providing an opportunity to measure the cavity resistance at low temperature. Figure 9 shows the cavity temperature during the period resistance measurements were made.

A sample of the measured voltage and current is shown in Fig.10.

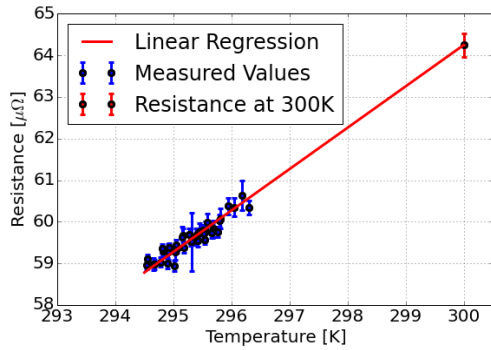


Figure 8: Cavity resistance extrapolated to 300 K.

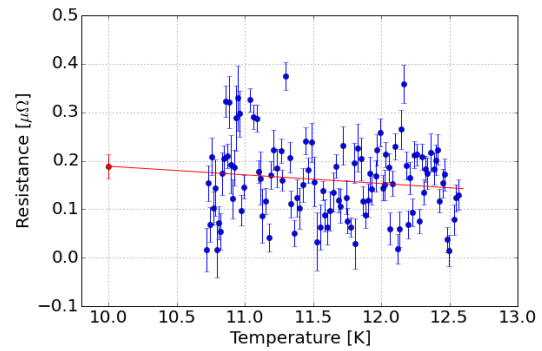


Figure 11: Resistance measurements at low temperature for DQW SPS1 crab cavity and extrapolation to 10 K

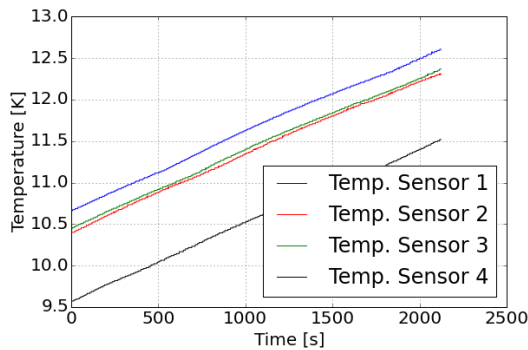


Figure 9: The temperature of the DQW SPS1 crab cavity measured over part of the thermal cycle during which the low temperature resistance measurements were made.

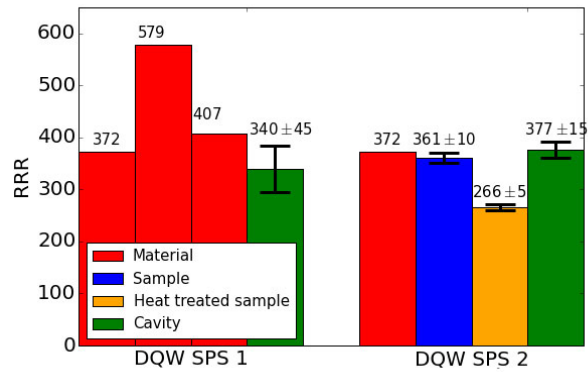


Figure 12: Comparison of: the RRR measured in situ on both cavities (green); with that of the non heat treated (blue) and heat treated (orange) samples made from the same material as the DQW SPS 2 cavity; and the RRR, as measured by the supplier, of the raw material used to form the cavities (red).

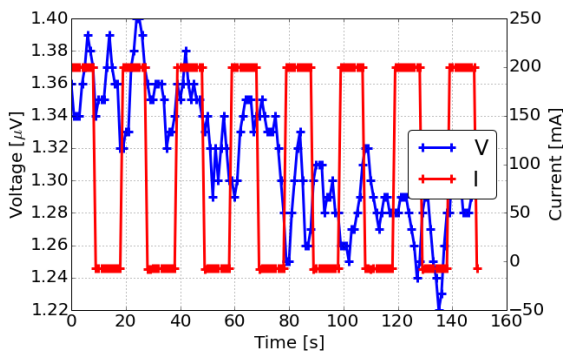


Figure 10: A sample of the current and voltage data recorded at 10K. Both the standard deviation between measurements and the long term drift dwarf the signal. Analysis is only possible by averaging over a very large number of individual measurements.

It can be seen that the size of both the noise and the ground drift is much larger than the signal, nevertheless it is possible to recover a signal by averaging a large number of measurements. Figure 11 shows the weighted means and standard deviations of the resistance measured at low temperatures and the extrapolation to 10 K. There is no discernible trend in the resistance with temperature which is to be expected at low temperatures where the resistance is dominated by the residual resistance. The RRR can be found as per Eqn.1.

### COMPARISON OF RRR MEASUREMENTS

The DQW SPS 1 cavity was made from three sheets with a RRR as measured by the supplier of the Niobium of 372, 579 and 407. The DQW SPS 2 cavity and the tested samples, were made from a single sheet which had a RRR as measured by the supplier of 372.

Figure 12 compares the RRR measured on the DQW SPS 1 and 2 cavities with the RRR of the measured samples and the RRR of the raw materials from which the cavities were formed as measured by the supplier.



The RRR measured on DQW SPS 1 cavity was lower than all of the original RRR values of the sheets from which it was manufactured. This suggests the RRR may have been degraded at some point during the fabrication process.

The DQW SPS2 cavity was made from a single sheet of Niobium with a RRR of 372. The RRR test done at CERN on a sample of this material agrees to within approximately 1 standard deviation of the measurement error as does the RRR of the cavity itself. However the RRR of the heat treated samples was significantly reduced. This is somewhat surprising as it suggests the RRR of the cavity was not greatly affected by the fabrication process even though the samples were strongly effected by part of it. A possible explanation for this is given in the conclusions.

The error on the cavity RRRs is greater than on the sample RRRs mainly due to the much lower resistance of the cavities. The DQW SPS 2 error is lower than that of the DQW SPS 1 cavity as a higher current was used.

## CONCLUSION AND FUTURE WORK

It has been shown that it is possible to measure the bulk RRR directly on the cavity during a cold test with an error of less than 15%.

The measured DQW SPS 2 RRR was in good agreement with the samples tested before heat treatment. However, the samples tested after receiving the same heat treatment as the cavity had a significantly lower RRR. This unexpected result demonstrates the value of measuring the cavity RRR in-situ. One possible explanation for this result is that, due to the smaller size of the samples and, the fact that the beam ports of the cavity were covered with Niobium during the heat treatment, the ratio of surface area exposed to the oven environment to volume is greater for the samples. Therefore any deleterious effect of the heat treatment is likely to be magnified.

Future cold tests of the UK4R crab cavity and other bare bulk Niobium cavities are planned for which the bulk RRR will also be measured. For these tests a new cable has been ordered which will permit larger currents of up to 6 A to be supplied to the cavity. This will increase the voltage drop across the cavity and enable more accurate measurements.

## ACKNOWLEDGEMENT

The authors would like to thank Rama Calaga, Konrad Eiler, Marco Garlasche, Paula Menendez and Sebastien Prunet for preparing and testing the samples in the cryolab, providing information on the material from which the cavities were manufactured and many useful discussions.

## REFERENCES

- [1] O. Brüning and L. Rossi, *The High Luminosity Large Hadron Collider*, Singapore: World Scientific Publishing, 2015.
- [2] O. Brüning *et al.*, *LHC Design Report*, Geneva, Switzerland: CERN, 2004.

- [3] R. Palmer, "Energy scaling, crab crossing and the pair problem", SLAC, California, U.S.A., Rep. SLAC-PUB-4707, Dec. 1988.
- [4] S. Verdú-Andres *et al.*, "Design and prototyping of HL-LHC double quarter wave crab cavities for SPS test", in *International Particle Accelerator Conference 2015. (IPAC2015)*, Richmond, VA, USA, May 2015, paper MOBD2, pp. 64–66.
- [5] S. Silva and J. Delayen, "Design evolution and properties of superconducting parallel-bar rf-dipole deflecting and crabbing cavities", *Phys. Rev. ST Accel. Beams*, vol. 16, p. 12004, Jan. 2013.
- [6] B. Hall, "Designing the Four Rod Crab Cavity for the High-Luminosity LHC upgrade", Ph.D. thesis, Eng. Dept., University of Lancaster, UK, 2012.
- [7] H. Park, "USLARP Crab Cavity Test Results", presented at International Review of the Crab Cavity Performance for HiLumi, Geneva, Switzerland, Apr. 2017, unpublished.
- [8] A. Castilla, "CERN Cavity Results", presented at International Review of the Crab Cavity Performance for HiLumi, Geneva, Switzerland, Apr. 2017, unpublished.
- [9] H. Padamsee, "Superconductivity essentials", in *RF Superconductivity for Accelerators*, New York, NY, USA: Wiley, 1998, pp. 57–76.
- [10] W. Jones and N. March, *Theoretical Solid State Physics*. London, UK: Wiley-Interscience, 1973.
- [11] G. Wiedemann and R. Franz, "Ueber die Wärme-Leitungsfähigkeit der Metalle", *Annalen der Physik*, vol. 165 (8), p. 497, 1853.
- [12] H. Safa, "Influence of the RRR of Niobium on the RF Properties of Superconducting Cavities", in *Advances in Cryogenic Engineering*, P. Kittel. Boston, MA, USA: Springer, 1998, pp. 71–76.
- [13] S. Patalwar *et al.*, "Key design features of the crab-cavity cryomodule for HI-LUMI LHC", in *International Particle Accelerator Conference 2014. (IPAC2014)*, Dresden, Germany, May 2014, paper WEPRI045, pp. 2580–2582.
- [14] Y. Jung, M. Hyun and M. Joung, "RRR characteristics for SRF cavities", *Journal of the Korean Phys. Soc.*, vol. 67 (8), p. 1319, Oct. 2015.
- [15] Lakeshore, <http://www.lakeshore.com/products/Cryogenic-Temperature-Sensors>
- [16] J. Vogt, O. Kugeler and J. Knobloch, "Impact of cool-down conditions at  $T_c$  on the superconducting rf cavity quality factor", *Phys. Rev. ST Accel. Beams*, vol. 16, p. 102002, Oct. 2013.